Depletion of Cytosolic Phospholipase A$_2$ in Bone Marrow–Derived Macrophages Protects against Lung Cancer Progression and Metastasis

Mary C.M. Weiser-Evans,[1] Xue-Qing Wang,[1] Jay Amin,[1] Vicki Van Putten,[1] Rashmi Choudhary,[1] Robert A. Winn,[2] Robert Scheinman,[3] Peter Simpson,[1] Mark W. Geraci,[2] and Raphael A. Nemenoff[1]

[1]Divisions of Renal Diseases and Hypertension and Pulmonary Sciences and [2]Critical Care Medicine, Department of Medicine, and [3]School of Pharmacy, University of Colorado Denver, Denver, Colorado

Abstract

Cancer progression and metastasis involves interactions between tumor cells and the tumor microenvironment (TME). We reported that mice deficient for cytosolic phospholipase A$_2$ (cPLA$_2$-KO) are protected against the development of lung tumors. The goal of this study was to examine the role of cPLA$_2$ in the TME. Mouse lung cancer cells (CMT167 and Lewis lung carcinoma cells) injected directly into lungs of syngeneic mice formed a primary tumor, and then metastasized to other lobes of the lung and to the mediastinal lymph nodes. Identical cells injected into cPLA$_2$-KO mice showed a dramatic decrease in the numbers of secondary metastatic tumors. This was associated with decreased macrophage staining surrounding the tumor. Wild-type mice transplanted with cPLA$_2$-KO bone marrow had a marked survival advantage after inoculation with tumor cells compared with mice receiving wild-type (WT) bone marrow. *In vitro*, coculturing CMT167 cells with bone marrow–derived macrophages from WT mice increased production of interleukin 6 (IL-6) by cancer cells. This increase was blocked in cocultures using cPLA$_2$-KO macrophages. Correspondingly, IL-6 staining was decreased in tumors grown in cPLA$_2$-KO mice. These data suggest that stromal cPLA$_2$ plays a critical role in tumor progression by altering tumor-macrophage interactions and cytokine production. [Cancer Res 2009;69(5):1733–8]

Introduction

Lung cancer is the leading cause of cancer deaths. At diagnosis, the majority of patients display metastases, and available treatments fail to prolong survival. During the past 25 years, researchers studying epithelial cancers have focused on genetic changes in tumor cells. However, it has become apparent that cancer progression and metastasis requires complex interactions between tumor cells and the surrounding stroma (1). We have studied the role of cytosolic phospholipase A$_2$ cPLA$_2$ in the development of lung cancer, focusing on tumor cells themselves. Activation of cPLA$_2$, resulting in arachidonic acid release, controls production of a family of eicosanoids, including prostaglandins. In non–small cell lung cancer (NSCLC) cells, oncogenic K-Ras leads to elevated levels of cPLA$_2$ and prostaglandin E$_2$ production; blocking this pathway inhibits transformed growth *in vitro* and in xenograft

models (2). However, little is known regarding the role of cPLA$_2$ in the tumor microenvironment (TME). Although global deletion of cPLA$_2$ in mice inhibits chemically induced lung tumorigenesis (3), these studies do not discriminate between the actions of cPLA$_2$ in tumor cells versus the TME. In this study, we used a model using mouse lung tumor cells injected into the lungs of syngeneic, immune-competent mice. These cells form well-defined primary tumors, which metastasize to other lobes of the lungs and into the mediastinal lymph nodes. Comparing tumor progression in wild-type (WT) versus cPLA$_2$-KO mice allowed us to specifically assess the role of this enzyme in the TME.

Materials and Methods

Cells. CMT167 cells obtained from Dr. Alvin Malkinson (School of Pharmacy, University of Colorado Denver, Denver, Colorado), and Lewis lung carcinoma cells were transfected with pGL3-Control Vector (Promega) containing firefly luciferase constitutively driven by an SV40 promoter and a vector containing neomycin resistance. Stable transfectants were selected using medium containing G418, and individual clones were screened for luciferase activity. A clone with high luciferase activity (CMT167/luc or LLC/luc) was used for injection into animals. Bone marrow–derived cells were isolated from femurs and tibias of WT and cPLA$_2$ knockout mice and cultured in the presence of M-CSF to promote macrophage maturation as previously described (4). After 3 to 7 d in culture, these cells have the morphology of macrophages, and were >95% F4/80 positive.

Mice. cPLA$_2$-KO mice (5) were backcrossed >10 generations to C57BL/6 mice in the Center for Laboratory Animal Care at the University of Colorado Denver. Wild-type littermates were used as controls in all studies. All procedures were performed under a protocol approved by the Institutional Animal Care and Use Committee at the University of Colorado Denver. For bone marrow transplant, donor mice were sacrificed, femurs and tibias were aseptically removed, and bone marrow were obtained by aspiration. Cells were suspended in sterile PBS + 1% FCS. Recipient WT and cPLA$_2$-KO mice were γ-irradiated (900–1,200 RAD split doses) by Cesium source at age 7 to 8 wk. Twenty-four h later, halothane anesthetized, irradiated recipients were injected with donor marrow via retro-orbital injection (5 × 10^6 BM MNC/mouse). UBI-EGFP mice were used as WT bone marrow donors to track bone marrow by green fluorescent protein (GFP) expression; cPLA$_2$-KO mice, without GFP-labeled bone marrow, were used for knockout bone marrow transplants.

Tumor cell injections. Mice were directly injected with the indicated tumor cells (10^5 per 40 μL), suspended in 10% Growth Factor Reduced Matrigel Matrix (BD Biosciences) PBS, through the rib cage into the left lobe of the lung using 30-g needles. For bioluminescence imaging, mice were injected i.p. with 300 mg/kg body weight luciferin before sedation and imaged using The IVIS Imaging System 50 Series (Caliper Life Sciences/Xenogen Corp.). At time of sacrifice, some lungs were inflated with India ink to better visualize and quantify additional large (>0.4 mm) and micro (<0.3 mm) secondary tumors. Tumor size was quantitated using digital calipers.
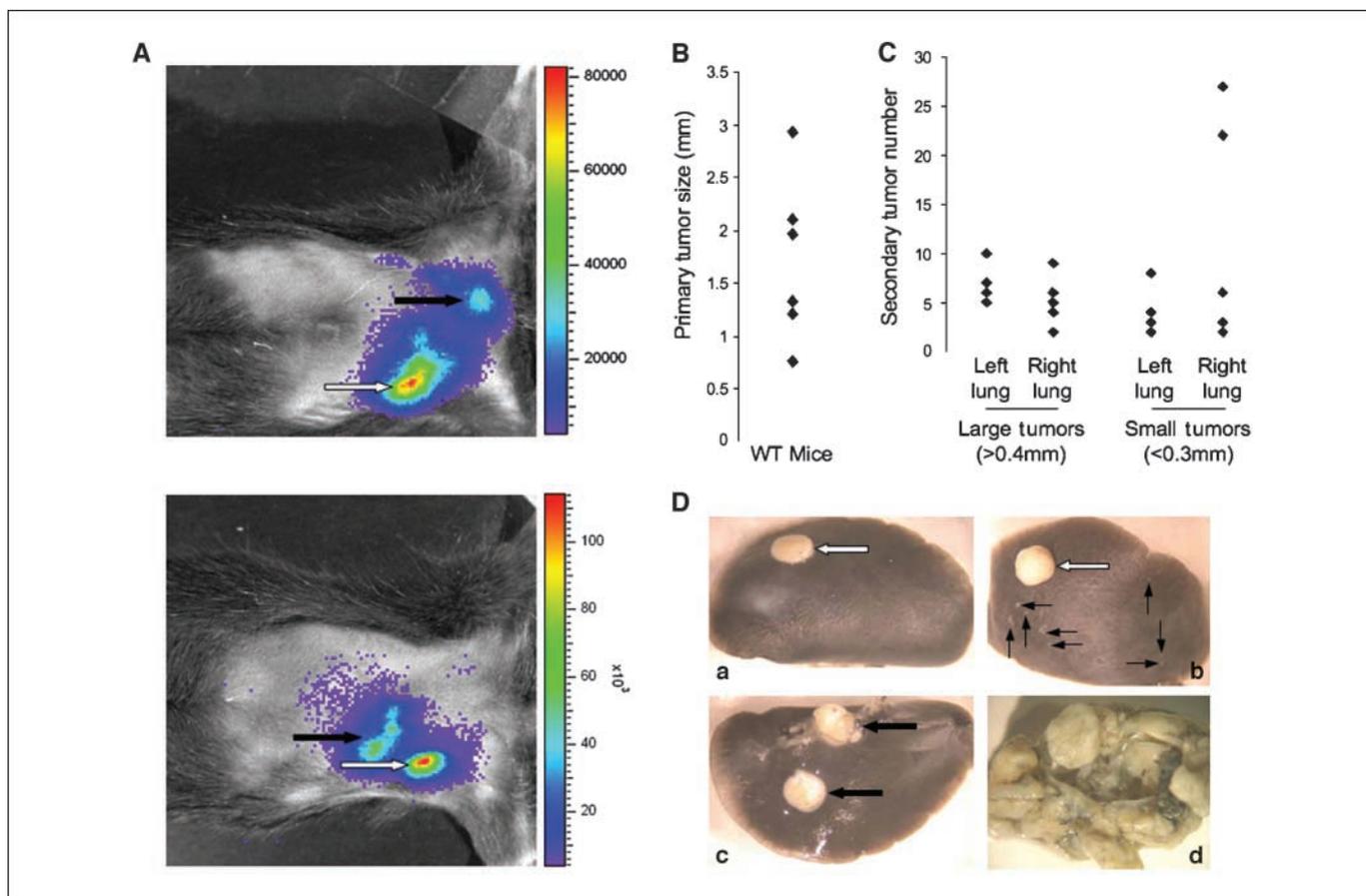
Cancer Research

Figure 1. Immune-competent lung cancer model. *A,* CMT/167 cells (10^5 per 40 µL of 10% Matrigel) were injected into the left lung lobe of WT mice. Four weeks after injection, mice were injected with luciferin and imaged for luciferase expression. *White arrows,* primary tumor; *black arrows,* secondary tumor metastases; two separate mice are shown. *B* and *C,* lungs from injected mice were harvested and inflated with India ink to identify tumors. Primary tumor diameter was measured by digital calipers. *B,* secondary tumors were identified, measured, and recorded as large (>0.4 mm) or micro (<0.3 mm; *C*). Individual points represent single animals. *D,* macroscopic images of injected lungs (*a–c*) and mediastinal lymph involvement (*d*). *White arrows,* primary tumors; *thick black arrows,* large secondary tumors; *thin black arrows,* microsecondary tumors.

Immunohistochemistry/fluorescence staining. For immunohistochemistry, formalin-fixed, paraffin-embedded tissues were deparaffinized, rehydrated, and underwent antigen retrieval by heating for 20 min at 115°C in a decloaking chamber (Biocare). Sections were then exposed to specific antibodies overnight at 4°C. Antigen/antibody complexes were visualized using kits from Vector Laboratories and sections lightly counterstained with hematoxylin. Negative controls included the use of mouse or rabbit IgG. Sections were visualized using an Olympus light microscope equipped with SPOT software. For double immunofluorescence labeling, tissue sections were treated as above. After incubations with primary antibodies, antigen/antibody complexes were visualized using rhodamine (Alexa Fluor-568)–coupled or FITC (Alexa Fluor-488)–coupled secondary antibodies (Molecular Probes); sections were sequentially incubated with specific primary and secondary antibodies. Coverslips were mounted with VectaShield medium containing 4′,6-diamidino-2-phenylindole to detect all cell nuclei (Vector Laboratories), and sections were visualized using a Nikon inverted fluorescence microscope equipped with Metamorph software. Antibodies used include polyclonal anti-F4/80 (1:100; Caltag), FITC-conjugated anti-GFP (1:100; Abcam), and polyclonal anti–interleukin 6 (IL-6; 1:2,000; Abcam).

Coculture. Bone marrow–derived macrophages were grown on the bottom of Transwell inserts. CMT/167 cells were grown on Transwell filters. After 24 h in coculture, cells were separated and each cell type was placed in fresh medium. Condition medium was collected after 24 h and assayed for IL-6 production by specific ELISA.

Results and Discussion

The CMT167 cell line derived from a spontaneous alveolar lung carcinoma of a C57BL/6 female mouse (6) was stably transfected with firefly luciferase (CMT167/luc) to allow bioluminescent imaging to be performed. CMT167/luc cells suspended in Matrigel were injected through the rib cage into the left lobe of the lung of C57/BL6 mice as previously described (7, 8), and tumor formation were analyzed as a function of time by bioluminescent imaging (Fig. 1*A*). At 3 weeks, mice consistently developed large primary tumors at the sight of injection (Fig. 1*A* and *B*). Lungs were inflated with India ink to visualize and quantify additional large (>0.4 mm) and micro (<0.3 mm) secondary tumors. Wild-type mice exhibited multiple secondary tumors throughout the left and right lung lobes (Fig. 1*C* and *D, a–c*). By 4 weeks postinjection, all mice showed clinical features of mediastinal lymph node metastasis (Fig. 1*D, d*).

To assess the role of cPLA$_2$ in the TME, equal numbers of CMT167/luc cells were injected into WT or cPLA$_2$-KO mice, and lungs were harvested after 4 weeks. Quantification of tumor metastases was limited to large secondary tumors visible under a dissecting microscope. Growth of the primary tumor was not significantly different between the two groups of mice (Fig. 2*A*). CMT167 cells injected into WT mice metastasized to other lung lobes and into mediastinal lymph nodes. However, CMT167 cells

growing in cPLA$_2$-KO mice showed fewer metastases and little lymph involvement; five of five WT mice, but only one of five KO mice, exhibited lung metastases and lymph involvement by macroscopic morphologic examination (Fig. 2B). To extend the generality of these findings, we performed similar experiments with Lewis lung carcinoma cells, another lung cancer cell line derived from C57BL/6 mice. These cells are more aggressive as reflected by more rapid proliferation of the primary tumor and increased numbers of secondary tumors. However, as with CMT167 cells, we observed no statistical difference in the size of primary tumors (data not shown), but a marked decrease in secondary tumor number (Fig. 2C) in cPLA$_2$-KO mice compared with WT. CMT167 cells were used for all subsequent studies.

Although numerous cell types comprise the TME, attention has focused on tumor-associated macrophages (TAM) as mediators of tumor progression and metastasis (9). Macrophages express high levels of cPLA$_2$, and produce proangiogenic cytokines. We showed that macrophage recruitment to the lung is impaired in cPLA$_2$-KO mice after an inflammatory stimulus (10). TAMs surrounding tumors were assessed by F4/80 staining. Tumors grown in WT mice showed abundant accumulation of TAMs surrounding developing tumors. In contrast, fewer TAMs were detected in tumors of KO mice (Fig. 2D).

Recruitment of bone marrow–derived circulating monocytes/ macrophages is associated with more aggressive, malignant tumors. To assess the role of cPLA$_2$ in bone marrow–derived cells on tumor progression, WT mice received bone marrow transplants from either WT or cPLA$_2$-KO mice. Animals were allowed to recover for 5 weeks, and then injected with CMT167/ luc cells. Mice transplanted with cPLA$_2$-KO bone marrow had a marked survival advantage over mice transplanted with WT bone marrow (Fig. 3A). In separate studies, bone marrow derived from either WT or cPLA$_2$-KO mice was transplanted into a limited number of either WT or cPLA$_2$-KO recipients to examine recruitment of bone marrow–derived macrophages to the tumor. These studies used UBI-EGFP/B6 transgenic mice, which express EGFP in all cells, as WT bone marrow donors. Lungs were harvested 4 weeks after CMT167/luc injection and analyzed histologically. Mice receiving cPLA$_2$-KO bone marrow, independent of genotype, exhibited less inflammatory infiltrate surrounding the primary tumor compared with mice receiving WT bone marrow (Fig. 3B). Mice receiving WT bone marrow were examined for EGFP and stained for F4/80. Both groups of mice receiving WT bone marrow showed large numbers of EGFP[+];F4/80^{+} cells surrounding the tumor (Fig. 3C) indicating recruitment of bone marrow–derived macrophages. In both groups of mice receiving cPLA$_2$-KO bone marrow, fewer F4/80-positive cells were detected, consistent with fewer macrophages. These data suggest that the stromal protective effects of cPLA$_2$ depletion are mediated in large part through bone marrow–derived cells, and

Figure 2. cPLA$_2$ in the TME is essential for lung cancer progression. 10^5 CMT167 cells were injected into 5 WT or 5 cPLA$_2$-KO mice as above. Lungs were harvested 4 wk after injection. *A,* primary tumor size (diameter) was measured by caliper. Each point represents a single animal. *B,* numbers of large secondary tumors on left and right lungs were determined. Each point represents a single animal. Four cPLA$_2$ KO mice had no secondary tumors. *C,* 10^5 LLC cells were injected into 4 WT or 4 cPLA$_2$-KO mice. Lungs were harvested as described above, and primary and secondary tumors were evaluated. *D,* lung sections from WT (*top*) and KO (*bottom*) mice injected with CMT/167 cells were immunohistochemically stained for F4/80, a macrophage marker (*brown reaction color*). *Arrow,* F4/80(+) cells in secondary tumors growing in WT mice. *Insets,* shown at higher magnification in middle.
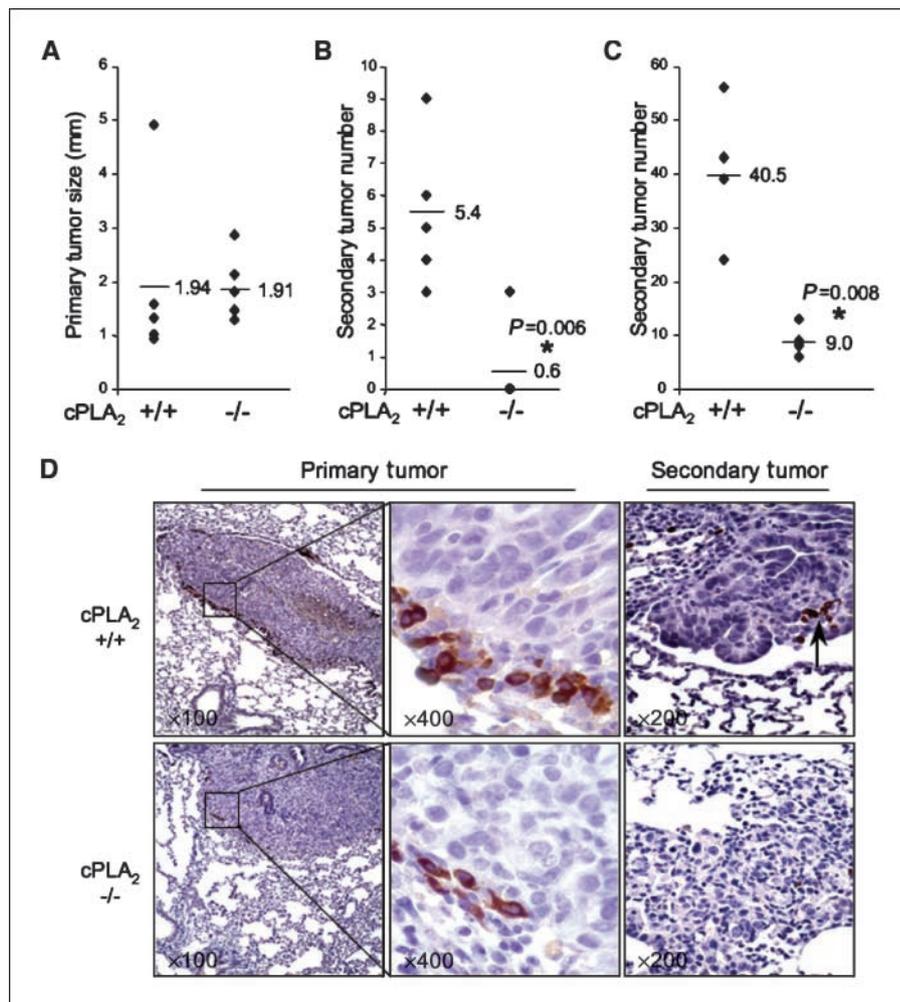
support a model in which $cPLA_2$ expression in bone marrow–derived macrophages is critical for recruitment of these cells to the site of the tumor.

Production of IL-6 by both tumor and stromal cells contributes to tumor progression as well as angiogenesis (11). To determine if $cPLA_2$ plays a role in IL-6 production *in vivo*, sections from tumors grown in WT or $cPLA_2$-KO mice were stained for IL-6. Tumors grown in $cPLA_2$-KO mice had markedly lower levels of IL-6 both within and surrounding the tumor, compared with tumors grown in WT mice (Fig. 4A). To examine IL-6 production *in vitro*, bone marrow–derived cells isolated from WT or $cPLA_2$-KO mice were cultured in the presence of M-CSF to promote macrophage maturation as previously described (4). These cells have the morphology of macrophages, and are >95% F4/80 positive. Macrophages derived from WT mice produced twice the levels of IL-6 compared with macrophages derived from $cPLA_2$-KO mice (Fig. 4B). Because interactions between cancer cells and macrophages effect cytokine production (12), IL-6 production was also assessed in cocultures of bone marrow–derived macrophages with CMT167 cells using Transwells, which allows diffusible mediators to act on each cell type. Coculture of macrophages with CMT167 cells increased IL-6 production in both WT and $cPLA_2$-KO macrophages, with WT macrophages continuing to produce twice the levels compared with $cPLA_2$-KO macrophages (Fig. 4B). CMT cells grown alone failed to produce detectable levels of IL-6. However, coculture with macrophages resulted in significant IL-6 production. Importantly, IL-6 production by CMT167 cocultured with $cPLA_2$-KO macrophages was only 40% of the levels seen with WT macrophage-CMT cell coculture (Fig. 4C).

Although $cPLA_2$ expression by NSCLC has been shown to be important for transformed growth (2), this is to our knowledge the first report indicating the importance of this enzyme in the TME. Our data indicate that two independent mouse lung cancer cell lines show a marked impairment in formation of secondary tumors when grown in $cPLA_2$-deficient mice. Although the TME comprises many types of cells, we have focused on the role of bone marrow–derived cells, specifically macrophages. Specific deletion of $cPLA_2$ in bone marrow–derived cells inhibits tumor progression and
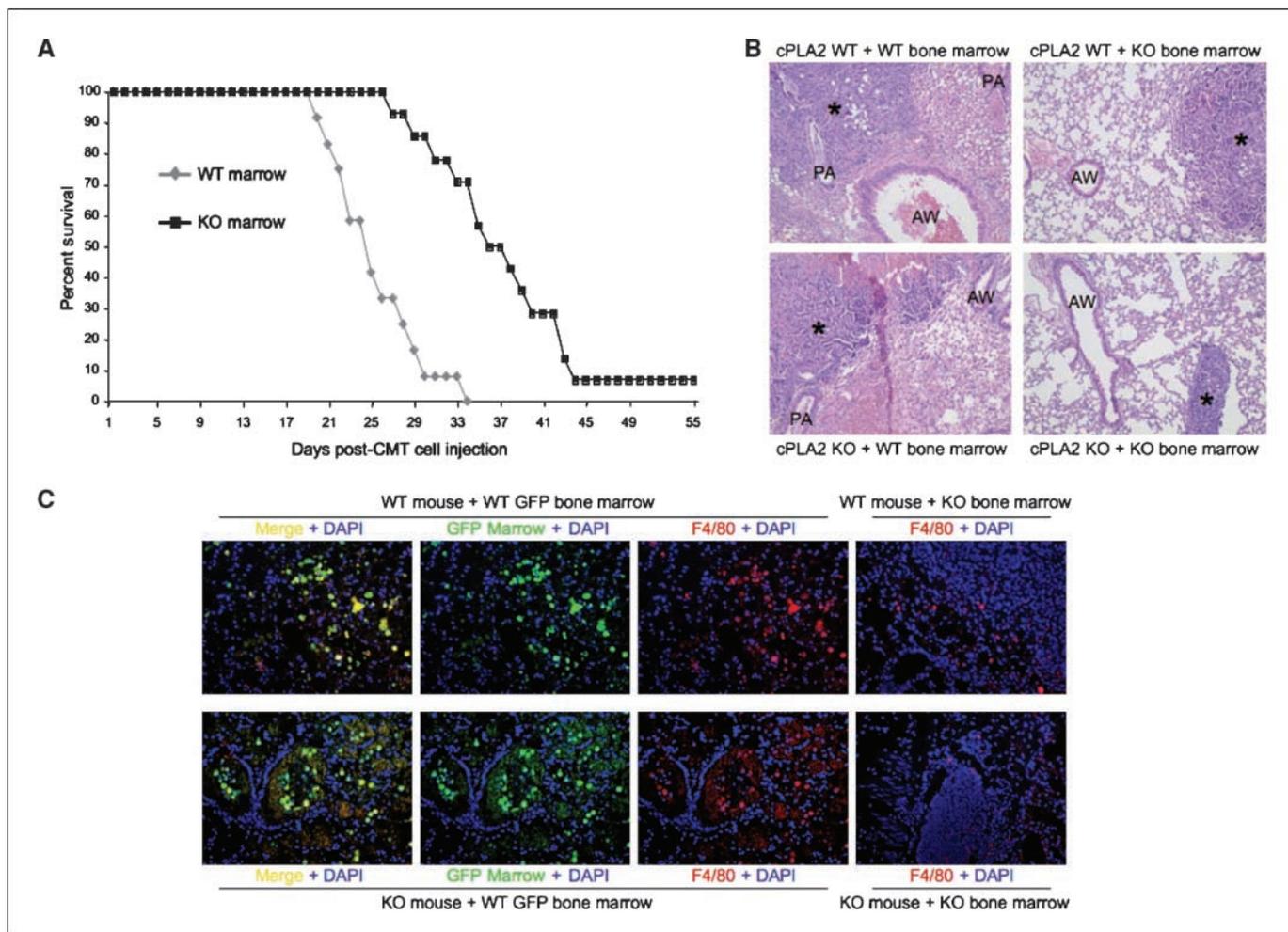

Figure 3. Increased survival and alterations in TAMs surrounding tumors grown in WT and $cPLA_2$-KO mice transplanted with $cPLA_2$ KO bone marrow. *A,* WT mice (*n* = 60) were lethally irradiated and transplanted with bone marrow from either UBI-EGFP/B6 WT or $cPLA_2$-KO mice. Five weeks after transplant, mice were inoculated with CMT167 cells. Kaplan-Meier survival curve of WT mice of the indicated bone marrow genotype is shown. *B,* H&E stain for tumors and surrounding stroma 4 wk after injection with CMT167 cells in either WT or $cPLA_2$-KO mice transplanted with the indicated bone marrow. *, primary tumor; *AW,* airway; *PA,* pulmonary artery. *C,* immunofluorescence for GFP and F4/80 in bone marrow–transplanted mice. Lung sections from the indicated mice transplanted with either WT or $cPLA_2$-KO bone marrow were examined for accumulation of macrophages (*F4/80*[+]) and bone marrow–derived cells (*GFP*[+]). Mice receiving UBI-EGFP/B6–derived WT bone marrow were examined for GFP (*green*) and stained for F4/80 (*red*). Double-positive cells were detected surrounding the primary tumor (*left, top*, and *bottom*). Mice receiving $cPLA_2$-KO bone marrow were stained for F4/80 to detect macrophages (*right, top*, and *bottom*).

Figure 4. cPLA$_2$ deficiency attenuates production of IL-6 in cocultures of CMT cells and bone marrow–derived macrophages. *A,* tumor-bearing lung sections from WT or cPLA$_2$-KO mice were immunohistochemically stained for IL-6 (*brown reaction color*). Representative images of tumors in WT and cPLA$_2$-KO mice are shown. *,* tumor. *B* and *C,* bone marrow–derived macrophages were prepared as described in the Materials and Methods from either WT or cPLA$_2$-KO mice. CMT/167 cells were placed in coculture with macrophages using Transwell filters. Control cultures contained either CMT/167 cells or macrophages with medium alone. After 24 h, cells in coculture were separated and all cells received fresh medium for an additional 24 h. Conditioned medium was then collected and assayed for IL-6 production; levels were normalized to cell protein. *B,* IL-6 production by macrophages; *C,* IL-6 production by CMT/167 cells. *,* $P < 0.05$ versus each cell type grown alone; **,** $P < 0.05$ versus coculture with WT macrophages. Note: production of IL-6 by CMT cells alone was undetectable.
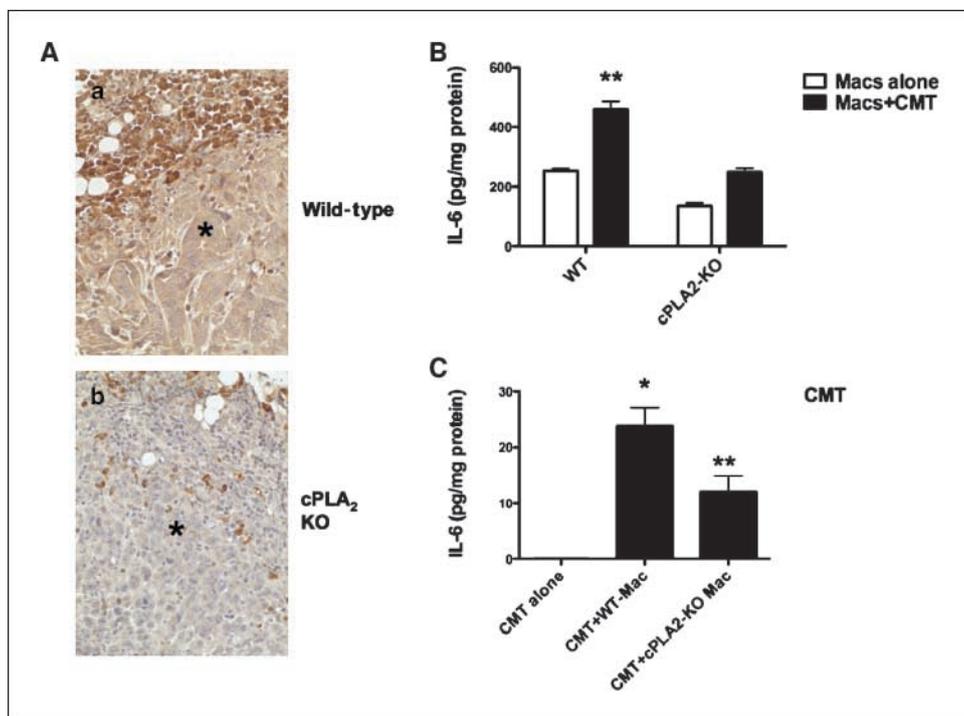
metastasis and promotes cancer survival. This protection is associated with decreased numbers of TAMs surrounding the tumors in cPLA$_2$-KO mice. In human lung cancer, increased numbers of macrophages surrounding the tumor has been associated with an unfavorable prognosis (13). Our findings are consistent with these observations.

Macrophages play a complex role in cancer progression. Although initially mediating cytotoxic effects on tumors, TAMs have been implicated in promoting tumor progression and metastasis. Production by TAMs of proangiogenic cytokines in cooperation with tumor cells stimulates tumor angiogenesis (14). TAMs secrete factors with immunomodulatory activity, inhibiting T-cell function and other immune antitumorigenic effects. IL-6, a critical cytokine for tumor progression, promotes cancer progression through effects on tumor cells or stroma (15). Our data indicate that tumors grown in cPLA$_2$-KO mice are exposed to lower levels of IL-6, associated with reduced tumor progression and metastasis. Consistent with this, *in vitro* data indicate that cPLA$_2$ contributes to IL-6 production by macrophages, and is critical for the synergistic induction of IL-6 seen in cocultures of cancer cells and macrophages.

The mechanism whereby cPLA$_2$ regulates IL-6 production remains to be established. cPLA$_2$ is critical for PGE$_2$ production, the major prostaglandin produced by macrophages and NSCLC cells. PGE$_2$ can induce IL-6 production in cholangiocarcinoma cells (16), and modulates cytokine production by macrophages leading to promotion of M2-type macrophages (17). PGE$_2$ can act as an

immune suppressor by inhibiting proliferation of T cells, effecting immunoglobulin production by B cells, and regulating dendritic cell maturation (18). Further studies will be required to define the role of PGE$_2$ in this model. Because cPLA$_2$ is critical for production of other eicosanoids, including leukotrienes, other mediators may contribute to the effects of stromal cPLA$_2$. In addition, our studies also do not rule out a role for cPLA$_2$ in other stromal cells, including fibroblasts and vascular cells. Recent studies have implicated production of PGE$_2$ by myeloid-derived suppressor cells as a mediator of breast cancer progression (19). Finally it should be noted that numerous studies have examined nonsteroidal anti-inflammatory drugs as therapeutic treatments for lung cancer. It seems that these agents may not only effect tumor growth but may also directly effect metastasis through targeting prostaglandin production in macrophages and other stromal cells (20).

Disclosure of Potential Conflicts of Interest

No potential conflicts of interest were disclosed.

Acknowledgments

References

1. Kenny PA, Lee GY, Bissell MJ. Targeting the tumor microenvironment. Front Biosci 2007;12:3468–74.
2. Heasley LE, Thaler S, Nicks M, Price B, Skorecki K, Nemenoff RA. Induction of cytosolic phospholipase A2 by oncogenic Ras in human non-small cell lung cancer. J Biol Chem 1997;272:14501–4.
3. Meyer AM, Dwyer-Nield LD, Hurteau GJ, et al. Decreased lung tumorigenesis in mice genetically deficient in cytosolic phospholipase A2. Carcinogenesis 2004;25:1517–24.
4. Riches DW, Henson PM, Remigio LK, Catterall JF, Strunk RC. Differential regulation of gene expression during macrophage activation with a polyribonucleotide. The role of endogenously derived IFN. J Immunol 1988;141:180–8.
5. Bonventre JV, Huang Z, Taheri MR, et al. Reduced

Cancer Research

fertility and postischaemic brain injury in mice deficient in cytosolic phospholipase A2. Nature 1997; 390:622–5.

6. Layton MG, Franks LM. Heterogeneity in a spontaneous mouse lung carcinoma: selection and characterisation of stable metastatic variants. Br J Cancer 1984;49: 415–21.

7. Chen X, Su Y, Fingleton B, et al. An orthotopic model of lung cancer to analyze primary and metastatic NSCLC growth in integrin alpha1-null mice. Clin Exp Metastasis 2005;22:185–93.

8. Onn A, Isobe T, Itasaka S, et al. Development of an orthotopic model to study the biology and therapy of primary human lung cancer in nude mice. Clin Cancer Res 2003;9:5532–9.

9. Condeelis J, Pollard JW. Macrophages: obligate partners for tumor cell migration, invasion, and metastasis. Cell 2006;124:263–6.

10. Meyer AM, Dwyer-Nield LD, Hurteau G, et al. Attenuation of the pulmonary inflammatory response

following butylated hydroxytoluene treatment of cytosolic phospholipase A2 null mice. Am J Physiol Lung Cell Mol Physiol 2006;290:L1260–6.

11. Naugler WE, Karin M. The wolf in sheep's clothing: the role of interleukin-6 in immunity, inflammation and cancer. Trends Mol Med 2008;14:109–19.

12. Hagemann T, Wilson J, Burke F, et al. Ovarian cancer cells polarize macrophages toward a tumor-associated phenotype. J Immunol 2006;176:5023–32.

13. Welsh TJ, Green RH, Richardson D, Waller DA, O'Byrne KJ, Bradding P. Macrophage and mast-cell invasion of tumor cell islets confers a marked survival advantage in non-small-cell lung cancer. J Clin Oncol 2005;23:8959–67.

14. Lewis CE, Pollard JW. Distinct role of macrophages in different tumor microenvironments. Cancer Res 2006; 66:605–12.

15. Ancrile B, Lim K-H, Counter CM. Oncogenic Ras-induced secretion of IL6 is required for tumorigenesis. Genes Dev 2007;21:1714–9.

16. Han C, Demetris AJ, Stolz DB, Xu L, Lim K, Wu T. Modulation of Stat3 activation by the cytosolic phospholipase A2α and cyclooxygenase-2-controlled prostaglandin E2 signaling pathway. J Biol Chem 2006;281: 24831–46.

17. Harizi H, Gualde N. Pivotal role of PGE2 and IL-10 in the cross-regulation of dendritic cell-derived inflammatory mediators. Cell Mol Immunol 2006;3: 271–7.

18. Harris SG, Padilla J, Koumas L, Ray D, Phipps RP. Prostaglandins as modulators of immunity. Trends Immunol 2002;23:144–50.

19. Sinha P, Clements VK, Bunt SK, Albelda SM, Ostrand-Rosenberg S. Cross-talk between myeloid-derived suppressor cells and macrophages subverts tumor immunity toward a type 2 response. J Immunol 2007;179:977–83.

20. Riedl K, Krysan K, Pold M, et al. Multifaceted roles of cyclooxygenase-2 in lung cancer. Drug Resist Updat 2004;7:169–84.

Cancer Research

AACR American Association for Cancer Research

Depletion of Cytosolic Phospholipase A₂ in Bone Marrow–Derived Macrophages Protects against Lung Cancer Progression and Metastasis

Mary C.M. Weiser-Evans, Xue-Qing Wang, Jay Amin, et al.

Updated version	Access the most recent version of this article at: doi:10.1158/0008-5472.CAN-08-3766

Cited articles	This article cites 20 articles, 9 of which you can access for free at: http://cancerres.aacrjournals.org/content/69/5/1733.full#ref-list-1
Citing articles	This article has been cited by 23 HighWire-hosted articles. Access the articles at: http://cancerres.aacrjournals.org/content/69/5/1733.full#related-urls

E-mail alerts	Sign up to receive free email-alerts related to this article or journal.
Reprints and Subscriptions	To order reprints of this article or to subscribe to the journal, contact the AACR Publications Department at pubs@aacr.org.
Permissions	To request permission to re-use all or part of this article, use this link http://cancerres.aacrjournals.org/content/69/5/1733. Click on "Request Permissions" which will take you to the Copyright Clearance Center's (CCC) Rightslink site.